EPJ Web of Conferences **36**, 00005 (2012)
DOI: 10.1051/epjconf/20123600005

Resonance production at SPS energies: CERES and NA49

O. Busch[1,a] for the CERES collaboration

[1] Universität Heidelberg, Germany

Abstract. We present results on resonance production by the NA49 and CERES collaborations. The measurement of the differential yields and spectral distributions of the $K^*(892)$, $\Delta(1232)$, ρ, ϕ and $\Lambda(1520)$ resonances from their leptonic and hadronic decay channels at different C.M.S. energies and for various colliding systems allows us to study in-medium modifications of the resonance mass, width and yield and constrains the properties of the hadronic phase. For $K^*(892)^0$, a strong system size dependence of the yield relative to kaon production is found. The production of the $\Delta(1232)$ resonance is consistent with thermal model expectations. ϕ meson spectra and yields reconstructed in the leptonic and hadronic decay channels are in agreement. Low-mass dilepton spectra indicate significant regeneration of the ρ meson and a strong modification of the ρ spectral function.

1 Introduction

Lattice QCD calculations predict a transition from confined hadronic matter to a chirally symmetric state of deconfined quarks and gluons at an energy density around 0.7 GeV/fm^3 [1] and a transition temperature of about 150-170 MeV [2]. Such conditions are believed to be reached in ultra-relativistic nucleus-nucleus collisions, where a transient state of high temperature and extreme energy density is created [3]. The system expands and cools and evolves into a hadron gas which finally decouples into the observed hadrons. Resonances created prior to chemical freeze-out (no more inelastic collisions) probe the evolution of the fireball to break-up at kinetic freeze-out (no more elastic collisions). They may interact with the medium in which they are produced and experience modifications of their mass, decay width and branching ratio relative to the 'vacuum' values measured in e^+e^- collisions [4–6]. Short-lived hadronic resonances with a lifetime similar to the fireball lifetime or smaller, are expected to decay and regenerate inside the medium: several generations probe different conditions of medium density and temperature. Furthermore, hadronic charged decay products may rescatter in the hadronic fireball stage [7], and thus their momenta do not allow to reconstruct this state in an invariant mass analysis. The interaction depends on the cross-section of the decay product with each particle in the fireball, the speed of each decay product relative to a typical fireball particle and, in particular, nuclear density. An analysis of the apparent yield relative to the expectation at chemical freeze-out constrains the properties of the hadronic phase.

There are various experimental parameters that can be varied. Via the choice of the resonance under study, the particle mass, quantum numbers (notably the strangeness content) and lifetime are determined. Some resonances can be reconstructed in hadronic and leptonic decay channels. Since leptons leave the fireball without further interactions and are not subject to rescattering, a comparison of resonance yields in the leptonic and hadronic decay channel can be used to study the rescattering effects. For the same reason, resonances reconstructed via leptonic decays probe the entire fireball history, whereas in the hadronic decay channel one might be more sensitive to resonances formed at a late stage of the fireball evolution with reduced density and rescattering probability (surface bias). Hence,

[a] e-mail: o.busch@gsi.de

in the leptonic decay channel a higher sensitivity to modifications of the mass and width in the early stage of the fireball is expected. Variation of the collision energy, and the size of the colliding nuclei allows to study different fireball sizes[1] and compare different freeze-out densities and temperatures.

In heavy-ion collisions enhanced strangeness production is found relative to p-p collisions. The enhancement was predicted to arise from gluon fragmentation into quark-antiquark pairs which is believed to have significantly lower threshold than strange-antistrange hadron pair production channels [10]. Statistical hadron gas models have been successfully employed to describe the measured particle yields at various collision energies [11–13]. In this hadron gas picture, enhanced production of strange particles in collisions of large nuclei arises as a consequence of the increased reaction volume, relaxing the constraints of local strangeness conservation. The comparison of yields of strangeness carrying resonances in nucleus-nucleus and p-p collisions needs to gauge a possible modification of the yield after chemical freeze-out against the expected strangeness enhancement.

In these proceedings, we give an overview of resonance production measured by the NA49 and the CERES experiments at the CERN SPS. In Sec. 2, we give a short description of the NA49 and CERES experiments and explain common features of the experimental signal extraction and correction procedures. In Sec. 3, results on $K^*(892)^0$ and $\bar{K}^*(892)^0$ production measured via the hadronic decay channel in central Pb-Pb, Si-Si, C-C and inelastic p-p at 158 AGeV ($\sqrt{s_{NN}}$ = 17 GeV) are summarized. In Sec. 4 we report measurements of Δ^{++} production in in Pb-Au collisions at 158 AGeV by the CERES experiment. CERES results on dilepton production in the invariant mass region of the ρ and below for Pb-Au collisions at 158 AGeV are presented in Sec. 5. The ϕ meson was reconstructed by CERES simultaneously in the hadronic and leptonic decay channel in Pb-Au collisions at 158 AGeV, and the NA49 collaboration has studied the beam energy dependence of ϕ production at SPS. These results are discussed in Sec. 6. We conclude with a summary and discussion in Sec. 7.

2 Experimental setup. Resonance reconstruction.

The NA49 experimental apparatus [14] at CERN is based on a fixed-target hadron spectrometer using heavy-ion beams from SPS accelerator. It consists of four large-volume time projection chambers (TPCs) for charged-particle tracking, two of which (VTPC) operate inside the magnetic field of two superconducting dipole magnets providing an excellent momentum measurement. Two larger main time projection chambers (MTPCs) are placed downstream, outside of the field. Charged-particle tracks are reconstructed from the charge deposited along the particle trajectories in the TPCs using a global tracking scheme which combines track segments from the same physical particle detected in different TPCs. The typical momentum resolution in Pb-Pb collisions is $\sigma(p)/p^2 = (0.3 - 7) \times 10^{-4} (GeV/c)^{-1}$ depending on track length.The interaction vertex is determined using the reconstructed tracks. In p-p collisions [15], additional information on the trajectory of the projectile from proportional chambers (BPDs) in the beam line was used for the vertex fit. Particle identification is based on measurements of the specific energy loss in the detector gas (dE/dx) of the TPCs The particle identification capabilities close to mid-rapidity are enhanced by a time-of-flight (TOF) scintillator system behind the MTPCs.

The CERES experiment [16–19] was conceived as a di-electron spectrometer. The Pb ions from the SPS impinge on a segmented Au target. The interaction vertex is reconstructed using charged particle track segments from two silicon drift detectors (SDD). Electrons are identified by their ring signature in two ring imaging Cherenkov (RICH) detectors, which are blind to hadrons below p ~4.5 GeV/c. The original experimental setup was upgraded by a downstream radial drift Time Projection Chamber (TPC) [19] in a magnetic field. The TPC allows to reconstruct hadrons over the full momentum range via particle tracking and improves the momentum resolution of the spectrometer (allowing e.g. to reconstruct the ϕ meson with a mass resolution of $\Delta m/m$=3.8%). The TPC also provides additional electron identification via measurement of the specific energy loss dE/dx. The spectrometer provides full azimuthal acceptance in the pseudorapidity range $2.1 < \eta < 2.65$.

Experimentally, in all cases considered in these proceedings, resonances are reconstructed via their decay into two charged particles. Since the decay daughters are not distinguishable from the other

[1] studies of the freeze-out volume via two-pion interferometry [8,9] show a strong centrality dependence and a comparably weak variation with collision energy

tracks in the heavy-ion environment, the signal is extracted on a statistical basis. All particle pairs of opposite charge are considered. In the invariant mass region of the signal, physically uncorrelated pairs contribute to the combinatorial background. The shape and level of this background can be determined experimentally constructing the invariant mass distribution from a priori uncorrelated pairs: combining like-sign pairs with equal charge[2], or combining tracks from different events. In the latter case, the mixed event background has to be normalized correctly to reproduce the level of background under the signal. After subtraction of the uncorrelated background contribution, typically a small residual background due to remaining correlations is observed. The signal is usually extracted from a combined fit to the signal plus background invariant mass distribution[3].

Unless mentioned otherwise, resonance yields and spectra are corrected for the branching ratio of the decay channel considered, detection efficiency, geometrical detector acceptance and in-flight decays, as well as vertex reconstruction efficiency in the case of p-p collisions.

Yields measured in nucleus-nucleus collisions can be compared to a reference (measured yields from elementary collisions or theoretical expectations) to judge potential effects of resonance regeneration or daughter rescattering. Here one remark is at order: in many cases, the resonance yield can not be measured down to zero momentum due to experimental constraints (geometrical acceptance, detection efficiency). In this case, the total yields are obtained extrapolating thermal fits to the data. Therefore, if a theory comparison on the level of differential spectra is not possible, conclusions based on total yields have to carefully consider the experimentally accessible phase space. On the part of the experiments, measured spectra are often compared to blast-wave fits [21], based on a simplified parametric hydrodynamical description of the particle emitting source.

3 $K^*(892)^0$ and $\bar{K}^*(892)^0$ production measured by NA49

The $K^*(892)^0$ resonance and its anti-particle are reconstructed via the $K^+\pi^-$ and $K^-\pi^+$ decay channels respectively, in central Pb-Pb, Si-Si, C-C and p-p collisions at 158 AGeV [22]. The measurements cover a wide rapidity interval close to midrapidity, $0.3<y<1.8$, and a transverse momentum range $0< p_t <2.0$ GeV/c (Pb-Pb).

Within the experimental uncertainties, no mass shift or modification of the width of the meson is observed in central Pb-Pb collisions. The transverse mass spectra yield inverse slope parameters (T=339 ±9 for $K^*(892)^0$ and T=329 ±12 for $\bar{K}^*(892)^0$) much larger than for kaons, but closer to the higher mass ϕ meson. Small deviations of the transverse mass differential yield from a purely exponential shape might be interpreted as signature of a momentum dependent attenuation of the K^* in the fireball, but are also reproduced by a blast wave fit.

In the left panel of Fig. 1 [22], we present the yield normalized to the number of wounded nucleons (participants, but excluding nucleons participating only in secondary interactions) in the four collision systems under study. This quantity seems to increase from p+p to C-C and Si-Si collisions and then decrease to central Pb-Pb, indicating possibly an interplay between strangeness enhancement in nucleus-nucleus collisions and the interaction of the $K^*(892)$ and its decay products in the produced fireball. In the ratios $\langle K^*(892)\rangle/\langle K^+\rangle$ and $\langle \bar{K}^*(892)\rangle/\langle K^-\rangle$ the effect of strangeness enhancement should approximately cancel, since kaons and $K^*(892)$ contain the same valence quarks. The strong system size dependence observed in these quantities, shown in the right hand panel of Fig. 1, indicates a sizeable effect of interactions in the fireball with destruction dominating regeneration.

4 $\Delta(1232)$ production measured by the CERES experiment

We present preliminary results on $\Delta(1232)^{++}$ production [23] in Pb-Au collisions at 158 AGeV from the CERES collaboration. The resonance is reconstructed in the $p\pi^+$ channel. The proton and pion

[2] the analog procedure is not possible for the reconstruction of of $\Delta(1232)$ in the $p\pi$ channel, since any combination of daughter charges corresponds to an existing resonance state of the isospin quadruplet.

[3] It is interesting to note that such residual background is not observed for the ϕ meson in the dilepton decay channel, in contrast to the K^+K^- decay, as discussed in Sec. 6. Spectra and yields measured simultaneously in both channels agree [20].

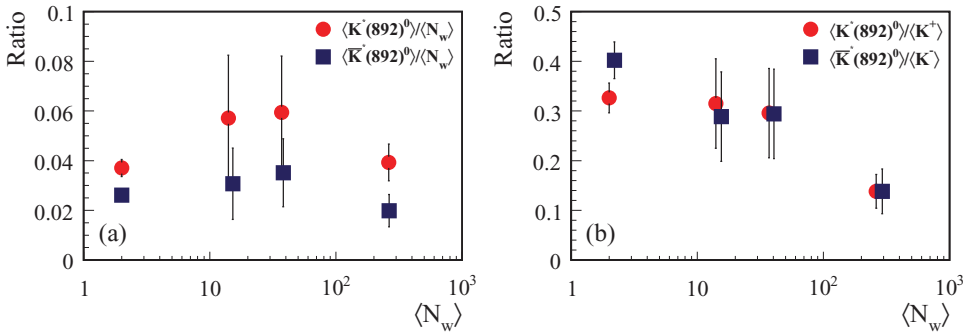

Fig. 1. (Color Online) $K^*(892)$ production measured by the NA49 experiment [22]. (a) $K^*(892)^0$ and $\bar{K}^*(892)^0$ yields per wounded nucleon versus size of the collision system. (b) ratios $\langle K^*(892)\rangle/\langle K^+\rangle$ and $\langle \bar{K}^*(892)\rangle/\langle K^+\rangle$ versus size of the collision system.

trajectories are reconstructed in the TPC and SDD detectors within $2.1< \eta <2.7$. Protons are identified using the TPC dE/dx information. For background rejection, a minimum transverse momentum of both daughters (p_t^p >0.1 GeV/c, p_t^π >0.15 GeV/c) are required and the pair opening angle is restricted to ($0.05< \Theta <0.46$). The uncorrelated background contribution is estimated from mixed events and subtracted. An example for the invariant mass distribution for one bin in p_t is shown in Fig. 2 (left panel). Experimental effects introduce a slight bias on the values of the reconstructed mass (~50 MeV) and width (~20 MeV), which can be reproduced by detector simulations using the nominal values as an input. Within experimental uncertainties, resonance mass and width are consistent with the PDG [24] values.

The raw yields are corrected for efficiency and acceptance. A dedicated investigation of the systematic uncertainties for this specific analysis was not carried out. The acceptance and efficiency correction factors and the signal extraction procedure are similar to the case of the ϕ meson reconstructed in the K^+K^- decay mode [20] described in Sec. 6. Therefore we estimate the systematic error to be of the order of 12%.

The transverse momentum spectrum in the rapidity interval $2.0< y^{\Delta} <2.4$ is shown in the right panel in Fig. 2. The distribution is well described by a thermal fit with a slope of 318±36 MeV. We find that the spectrum can also be well reproduced by a blast-wave fit. The total yield of $\Delta(1232)^{++}$ is dN/dy =5.4±0.91(stat) ±0.65(syst) for the 7% most central events. Using a negative hadron multiplicity N_{h^-} ($2.0<y_\pi <2.4$) of 66.4±0.8 as in [20], the measured ratio Δ^{++}/h^- = 34.5±5.8(stat) ±4.1(syst) $\cdot 10^{-3}$ is consistent with the thermal model predictions Δ^{++}/h^- = $47.6\cdot 10^{-3}$ [12] within statistical and systematic uncertainties. In the momentum range covered by the measurement, no indication for resonance absorption or regeneration or rescattering is found.

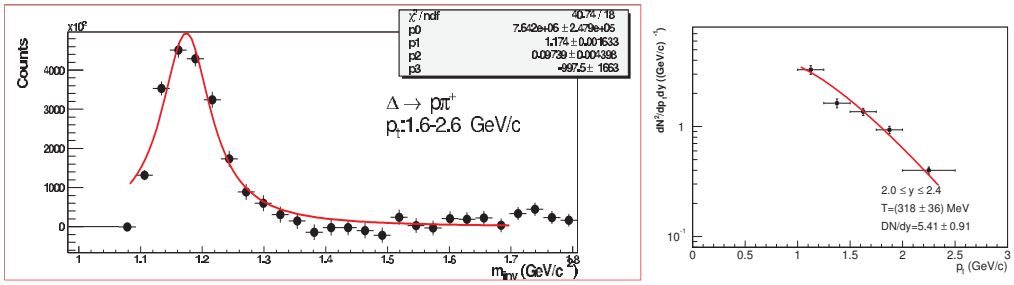

Fig. 2. (Color Online) $\Delta(1232)^{++}$ reconstruction in CERES (preliminary). Left panel: example for the $p\pi^+$ invariant mass distribution. The insert shows the fitted values of mass (fit parameter p1) and width (p2) in units of GeV/c^2. Right panel: $\Delta(1232)^{++}$ transverse momentum spectrum for $2.0< y^{\Delta} <2.4$. The line indicates a thermal fit.

5 Low-mass electron-positron pairs from CERES

The CERES collaboration has measured e^+e^- pair production at SPS for various collision systems and beam energies [25–28]. In these proceedings, we focus on results for central (σ/σ_{geo}=7%) Pb-Au collisions at 158 AGeV [29]. Electron legs are reconstructed in the pseudorapidity range 2.1< η <2.65. To suppress background from conversion electrons, a minimum single track transverse momentum p_t > 0.2 GeV/c and a minimum pair opening angle of 35 mrad are required. The e^+e^- signal pair yield is corrected for electron reconstruction efficiency and normalized to the average charged particle multiplicity $\langle N_{ch} \rangle$.

In Fig. 3(a), the e^+e^- invariant mass distribution is compared with the 'hadronic cocktail', which comprises the yield from hadronic decays in A-A collisions after chemical freeze-out [28]. In the mass region 0.2< m_{ee} <1.1 GeV/c^2, the data are enhanced over the cocktail by a factor 2.45±0.21(stat) ±0.35(syst) ± 0.58(decays). The improved mass resolution of the spectrometer after the upgrade with a radial TPC [19] provides access to the resonance structure in the ρ/ω and ϕ region (see Sec. 6).

In Fig. 3(b), the data are compared with model calculations incorporating enhanced dilepton production via thermal pion annihilation and a realistic space-time evolution [30]. The calculated dilepton yield was filtered by the CERES acceptance and folded with the experimental resolution. Temperature and baryon density dependent modifications of the ρ-spectral function have been taken into account: the dropping mass scenario which assumes a shift of the in-medium ρ mass [4,31], and the broadening scenario where the ρ spectral function is smeared due to coupling to the hadronic medium [6,32] (see also Fig. 4). The calculations for both spectral functions describe the enhancement reasonably well for masses below 0.7 GeV/c^2. In the resonance region, however, there is a notable difference between the calculations. In particular, in the mass region between the ω and the ϕ, the data clearly favor the broadening scenario over the dropping mass scenario.

In order to exhibit the shape of the in-medium contribution, we subtract the hadronic cocktail (excluding the ρ meson) from the data (Fig. 4). The vacuum ρ-decay contribution to the data ('cocktail ρ') is completely negligible compared to the measurements, indicating significant ρ resonance regeneration in the fireball. The excess data exhibit a very broad structure reaching low masses and exceed the vacuum ρ contribution by a factor 10.6±1.3. The data are compared to model calculations. Yield and spectral shape are well described by the broadening scenario but are not consistent with a dropping ρ mass: while the dropping mass calculation yields a rather narrow distribution, peaked at around 0.5 GeV/c^2, the measured excess is spread over a significantly wider mass range.

The measurement of the ρ spectral function in the di-electron channel provides access to very low invariant masses. In this mass regime, a particular mechanism contributes strongly to the di-electron yield: the strong coupling of the ρ to baryons in the hot and dense medium via "Rhosobar" excitations ($\rho \rightarrow BN^{-1}$). The importance of this mechanism is demonstrated in Fig. 4(b), where the data are

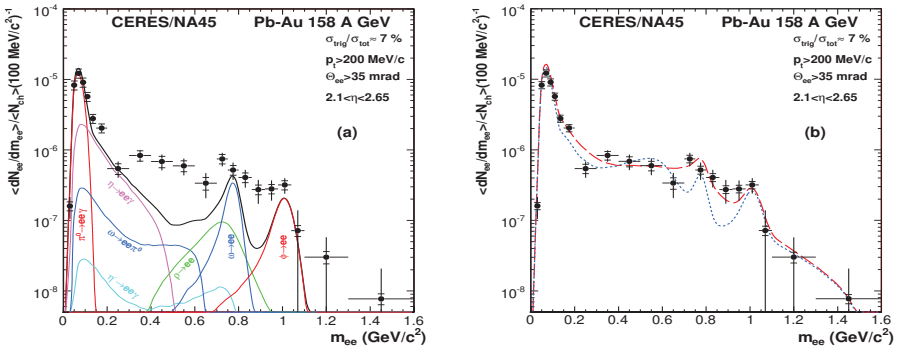

Fig. 3. (Color Online) (a) Invariant e^+e^- mass spectrum compared to the expectation from hadronic decays. (b) The same data compared to calculations including a dropping ρ mass (dashed) and a broadened ρ-spectra function (long-dashed). Figure from [29].

compared to in-medium hadronic spectral function calculations with and without baryon-induced interactions. The calculation omitting baryon effects falls short of the data for masses below 0.5 GeV/c^2, while the inclusion of baryon interactions describes the low-mass yield very well, providing strong evidence that the observed modifications of the ρ-spectral function are foremost due to interactions with the dense baryonic medium.

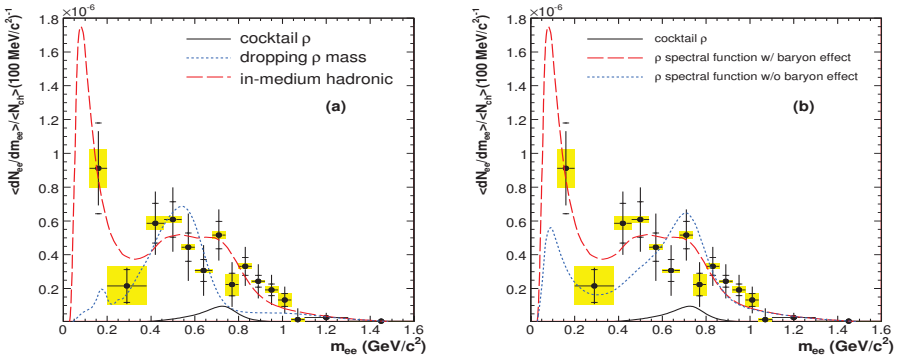

Fig. 4. (Color Online) e^+e^- pair yield after subtraction of the hadronic cocktail. The broadening scenario is compared to a calculation assuming a density dependent dropping ρ mass (a) and to a broadening scenario excluding baryon effects (b). Figure from [29].

6 ϕ meson production measured by CERES and NA49

The electron and hadron reconstruction capabilities of the CERES experiment allow for simultaneous reconstruction of the leptonic (e^+e^-) and charged kaon (K^+K^-) decay modes of the ϕ meson in the 7% most central Pb-Au collisions [20]. To study the ϕ meson in the K^+K^- decay mode, charged tracks are reconstructed in the TPC and combined to pairs. For the di-electron decay channel, electrons are identified using the RICH detectors and the *dE/dx* signal in the TPC. In the dilepton channel, the ρ meson could extend into the invariant mass range of the ϕ if its spectral function is modified in the medium. This physical background, along with a contribution due to QGP radiation, is estimated from theoretical models [6, 33, 34] and subtracted.

In Fig. 5, left panel, the ϕ meson yield for both decay modes as a function of transverse momentum are presented. The dilepton data are scaled to the acceptance of the hadronic channel. The ϕ meson yields and inverse slope parameters (T=273±9(stat)±10(syst) MeV) obtained in both decay modes agree within the experimental uncertainties. It should be noted that because of the long lifetime of the ϕ meson (τ = 47 fm) only a fraction decays inside the fireball. Thus, only a fraction of the ϕ mesons can be expected to be influenced by the surrounding medium.

In the NA49 experiment, the ϕ meson was reconstructed in the K^+K^- channel in central Pb-Pb collisions at 20, 30, 40, 80 and 158 AGeV/c, using charged Kaons identified in the MTPC [35], for rapidity intervals varying from 0<y<1.0 (158 AGeV/c) to 0<y<1.8 (20 AGeV/c). At all energies, the width and mass of the ϕ meson is consistent with the free-particles values. No indication for a mass shift or broadening is observed. The transverse momentum spectra obtained for the five beam energies are shown in Fig. 5, right panel. The spectrum obtained for 158 AGeV is compared to the results from the CERES experiment, after scaling the CERES data to account for small differences in acceptance and centrality. The results agree within errors, as do the total yields. In all cases, the data are well described by thermal fits, showing no sign of decay daughter rescattering. The measured yields for all energies can be described by a statistical hadron gas model with strangeness undersaturation, indicating consistently that the abundances of ϕ mesons are unchanged with respect to the values at chemical freeze-out.

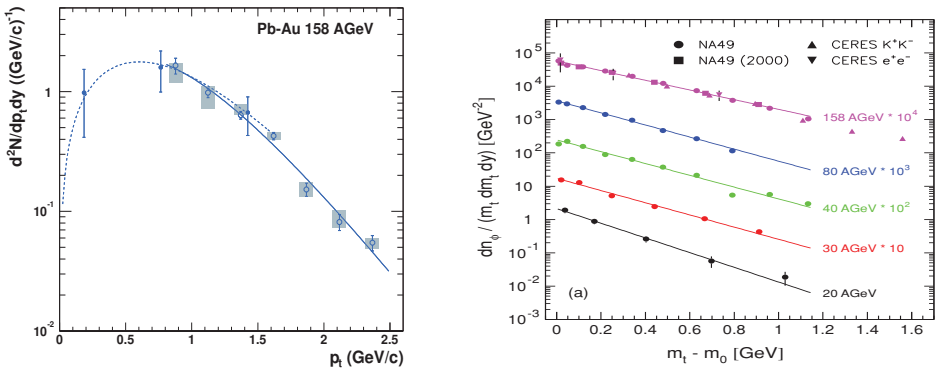

Fig. 5. (Color Online) ϕ meson reconstruction in CERES and NA49. Left panel: transverse momentum spectrum of ϕ mesons reconstructed by the CERES experiment in the e^+e^- decay mode (circles) and in the K^+K^- decay channels (triangles) [20]. Right panel: ϕ transverse mass spectra from NA49 for different collision energies [35].

7 Summary and discussion

Production of the K^*, Δ, ρ, and ϕ resonances in nucleus-nucleus collisions at SPS energies was studied by the NA49 and CERES collaborations. The results from NA49 for K*(892), ϕ, and preliminary results for $\Lambda(1520)$ [36] are summarized in Fig. 6 from [22]. The measured yields relative to the expectation from a Hadron Gas Model [13] are plotted versus the respective lifetimes (3.91, 12.7 and 46.5 fm/c). The suppression with respect to the model predictions seems to get stronger with decreasing lifetime of the resonance. This suggests that a large part of the reduction of the K^* yield may be caused by rescattering of its decay daughters during the hadronic stage of the fireball and implies that this stage lasts for a time at least comparable to the lifetime of the resonance. From two-pion interferometry, the total lifetime of the system to kinetic freeze-out is estimated to about 6 fm/c [9] to 8 fm/c [8] with a duration of emission of 2-3 fm/c.

Despite its large width / short lifetime (1.7 fm/c), no significant modification of the Δ resonance yield was observed by the CERES collaboration in the measured momentum range. It is interesting to note that similar observations were made at in Au-Au collisions at $\sqrt{s}$=200 GeV [37] (despite the different fireball composition at both energies [38]). The authors interpret a small rise of the ratio of Δ^{++}/p yields for more central collisions as a hint for resonance regeneration and the dependence of regeneration and rescattering.

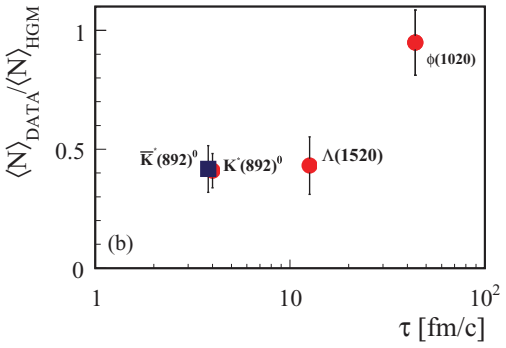

Fig. 6. (Color Online) Ratio of measured yields in central Pb-Pb collisions to the statistical hadron gas model prediction for $K^*(892)$, ϕ meson, and preliminary measurements for $\Lambda(1520)$ versus the lifetime τ of the resonance state. Figure from [22].

The CERES results for the ρ (lifetime 1.3 fm/c) show a clear indication for resonance regeneration in the fireball and modification of the spectral shape. The data are described by coupling of the ρ to the hadronic medium in a thermal fireball model. The dominant contribution to the dilepton radiation emanates from matter close to the expected QGP phase boundary.

References

1. F. Karsch, E. Laermann, A. Peikert, Nucl. Phys. B**605** (2001) 579.
2. Y. Aoki, Z. Fodor, S.D. Katz, K.K. Szabó, Phys. Lett. B**643** (2006) 46;
   S. Borsányi *et al.* arXiv:1005.3508 [hep-lat].
3. P. Braun-Munzinger, J. Stachel, Nature **448** (2007) 302.
4. G.E. Brown, M. Rho, Phys. Rev. Lett. **66** (1991) 2720;
   G.E. Brown, M. Rho, Phys. Rep. **269** (1996) 333.
5. T. Hatsuda, S. Lee, Phys. Rev. C**46** (1992) R34.
6. R. Rapp, J. Wambach, Adv. Nucl. Phys. **25** (2000) 1.
7. G. Torrieri, J. Rafelski, Phys. Lett. B**509**, (2001) 239.
8. D. Adamová *et al.*, Nucl. Phys. A**714** (2003) 124.
9. C. Alt *et al.*, Phys. Rev. C**77** (2008) 064908.
10. J. Rafelski, B. Müller, Phys. Rev. Lett. **48**, (1982) 1066.
11. P. Braun-Munzinger, I. Heppe, J. Stachel, Phys. Lett. B**465**(1999) 15.
12. A. Andronic, P. Braun-Munzinger, J. Stachel, Nucl. Phys. A**772** (2006) 167.
13. F. Beccattini, J. Manninen, M. Gaździcki, Phys. Rev. C**73** (2006) 044905.
14. S. Afansiev *et al.*, Nucl. Instrum. Methods Phys. Res. Sect. A**430**, (1999) 210.
15. C. Alt *et al.*, Eur. Phys. J. C**45**, (2006) 343.
16. R. Baur *et al.*, Nucl. Instrum. Methods Phys. Res. A**371** (1996) 16.
17. P. Holl, P. Rehak, F. Ceretto, U. Faschingbauer, J.P. Wurm, A. Castoldi, E. Gatti, Nucl. Instrum. Methods Phys. Res. A**377** (1998) 367.
18. R. Baur *et al.*, Nucl. Instrum. Methods Phys. Res. A**343** (1994) 87.
19. D. Adamová *et al.*, Nucl. Instrum. Methods Phys. Res. A **593** (2008) 203.
20. D. Adamová *et al.*, Phys. Rev. Lett. **96**(2006) 152301.
21. F. Retiere, M. A. Lisa, Phys. Rev. C**70**, 044907.
22. T. Antitic *et al.*, Phys. Rev. C**84** (2011) 064909.
23. R. Ortega, private communication.
24. J. Beringer et al. (Particle Data Group), Phys. Rev. D86, 010001 (2012)
25. G. Agakichiev *et al.*, Eur. Phys. J. C**4**(1998) 231.
26. G. Agakichiev *et al.*, Phys. Rev. Lett. **75** (1995) 1272.
27. S. Damjanovic, Electron-pair production in Pb-Au collisions at 40 AGeV, PhD thesis, Ruprecht-Karls-Universität Heidelberg, 2002.
   www.physi.uni-heidelberg.de/physi/ceres/theses.html
28. G. Agakichiev *et al.*, Eur. Phys. J. C**41** (2005) 475.
29. D. Adamová *et al.*, Phys. Lett. B**666** (2008) 425.
30. R. Rapp, J. Wambach, Eur. Phys. J. A**6** (1999) 415.
31. G.E. Brown, M. Rho, Phys. Rep. **363** (2002) 85.
32. H. van Hees, R. Rapp, Phys. Rev. Lett **97** (2006) 102301.
33. E. Braaten, R.D. Pisarkski, T.-C. Yuan, Phys. Rev. Lett. **64** (1990) 2242.
34. K. Gallmeister *et al.*, Nucl. Phys. A**688** (2001) 939.
35. C. Alt *et al.*, Phys. Rev. C**78**(2008) 044907.
36. V. Friese *et al.*, Nucl. Phys. A**698** (2002) 487.
37. C. Markert *et al.*, J. Phys. G**31** (2005) S897.
38. D. Adamová *et al.*, Phys. Rev. Lett. **90**, 022301.